# Co-precipitation of Phosphate and Iron Limits Mitochondrial Phosphate Availability in *Saccharomyces cerevisiae* Lacking the Yeast Frataxin Homologue (*YFH1*)*

**Alexandra Seguin**[‡], **Renata Santos**[‡], **Debkumar Pain**[§], **Andrew Dancis**[¶], **Jean-Michel Camadro**[‡], **and Emmanuel Lesuisse**[‡1]

*From the* ‡*Institut Jacques Monod, CNRS-University Paris Diderot 75205 Paris cedex 13, France, the* §*Department of Pharmacology and Physiology, University of Medicine and Dentistry of New Jersey, Newark, New Jersey 07103, and the* ¶*Department of Medicine, University of Pennsylvania, Philadelphia, Pennsylvania 19104*

***Saccharomyces cerevisiae* cells lacking the yeast frataxin homologue (Δ*yfh1*) accumulate iron in the mitochondria in the form of nanoparticles of ferric phosphate. The phosphate content of Δ*yfh1* mitochondria was higher than that of wild-type mitochondria, but the proportion of mitochondrial phosphate that was soluble was much lower in Δ*yfh1* cells. The rates of phosphate and iron uptake *in vitro* by isolated mitochondria were higher for Δ*yfh1* than wild-type mitochondria, and a significant proportion of the phosphate and iron rapidly became insoluble in the mitochondrial matrix, suggesting co-precipitation of these species after oxidation of iron by oxygen. Increasing the amount of phosphate in the medium decreased the amount of iron accumulated by Δ*yfh1* cells and improved their growth in an iron-dependent manner, and this effect was mostly transcriptional. Overexpressing the major mitochondrial phosphate carrier, *MIR1*, slightly increased the concentration of soluble mitochondrial phosphate and significantly improved various mitochondrial functions (cytochromes, [Fe-S] clusters, and respiration) in Δ*yfh1* cells. We conclude that in Δ*yfh1* cells, soluble phosphate is limiting, due to its co-precipitation with iron.**

Friedreich ataxia is the most common hereditary recessive ataxia. The gene responsible for this neurodegenerative disease was cloned in 1996 (1). The corresponding protein (frataxin) is a small, highly conserved mitochondrial protein. It is now generally accepted that frataxin (Yfh1 in yeast) is one of the components of the mitochondrial [Fe-S] cluster machinery, acting either as an iron donor or more generally as a chaperone interacting with the desulfurase/scaffold proteins involved in [Fe-S] assembly (2, 3). However, it has proved to be more difficult to determine the precise role of frataxin than of other components of the [Fe-S] cluster machinery, partly

because the phenotypes associated with a lack of frataxin are both very diverse and differ according to the cellular model studied (for recent reviews, see Refs. 4 and 5). Indeed, the absence of frataxin results in direct or indirect defects in many pathways other than [Fe-S] biogenesis, including heme synthesis (6, 7), oxidative stress defense (8–10), apoptosis (11), and mitochondrial iron homeostasis (12). One major difficulty in studying the role of frataxin in the yeast model is to distinguish phenotypes that specifically result from the lack of frataxin from phenotypes shared by several mutants affected in [Fe-S] cluster biogenesis (13).

Frataxin-deficient yeast cells, like other mutants defective in [Fe-S] cluster biogenesis, accumulate huge amounts of iron in their mitochondria (14). The mechanisms of iron import, export, and storage in the mitochondria are still very poorly understood. Several proteins in *Saccharomyces cerevisiae* mitochondria have been proposed as candidate iron transporters. The proteins include the paralogous proteins Mmt1 and Mmt2 (15), and the paralogous mitochondrial carrier proteins Mrs3 and Mrs4 (16). The Mrs proteins (homologous to the mammalian mitoferrin) are the best candidates for the function of mitochondrial iron import (17–19). However, the mechanism of uptake is still completely unknown and will probably remain so as long as the iron substrate used by these proteins *in vivo* is not known. In Δ*yfh1* mitochondria, iron accumulates in the form of amorphous nanoparticles of ferric phosphate (6), and there is now evidence that the same is true for other mutants defective in [Fe-S] cluster biogenesis or export (13, 20, 21). Iron precipitated in this form is unavailable for biological processes, and thus, Δ*yfh1* cells might paradoxically suffer from iron deficiency despite being overloaded with iron (13). The effects of frataxin deficiency on iron metabolism in yeast have been studied extensively (reviewed in Ref. 4). But, as iron precipitates in the form of ferric phosphate in the mitochondria of Δ*yfh1* cells, the physiological consequences of iron accumulation/precipitation in these cells probably involve dysfunctions in both iron and phosphate metabolism. Like iron, the precipitated phosphate is probably unavailable for biological processes. Frataxin-deficient cells are very often studied with regards to disruption in iron homeostasis but were never studied with regards to disruption in phosphate homeostasis. However, the question of ferric phosphate accumulation in the mitochondria of some mu-

[1] To whom correspondence should be addressed: Lab. of Mitochondria, Metals, and Oxidative Stress, Institut Jacques Monod, CNRS-Université Paris Diderot, Bâtiment Buffon, 15 rue Hélène Brion, 75205 Paris cedex 13, France. Tel.: 33-1-5727-8028; Fax: 33-1-5727-8101; E-mail: lesuisse.emmanuel@ijm.univ-paris-diderot.fr.

tants can obviously be studied from both ends: iron and phosphate. In the present study, we decided to study this issue by focusing on phosphate rather than iron. Inorganic phosphate, which is vital for oxidative phosphorylation, is transported to the mitochondrial matrix by two partly redundant carriers, Mir1 and Pic2 (22, 23). Interestingly, Mir1 is also involved in protein import into mitochondria (24), and Pic2 can reversibly change its transport mode (antiport-uniport) according to the redox conditions (25). More generally, phosphate is involved in the homeostasis of several cations in different cellular compartments (26). Co-precipitation of phosphate with iron in $\Delta yfh1$ mitochondria is thus expected to have physiological implications. We therefore investigated the effects of phosphate precipitation in mitochondria of frataxin-deficient yeast cells. As far as we are aware, this is the first report addressing frataxin deficiency from this particular point of view.

## EXPERIMENTAL PROCEDURES

*Yeast Strains and Growth Conditions*—The strains used in this study were YPH499 (wild-type; MAT**a** *ura3-52 lys2-801 ade2-101 trp1-Δ63 his3-Δ200 leu2-Δ1 cyh2*), YPH499Δ*yfh1* (Δ*yfh1*; Δ*yfh1::TRP1*), YPH499Δ*mrs3*Δ*mrs4* (*mrs4::kanMX4*, *mrs3::URA3*), YPH499Δ*ggc1* (*ggc1::kanMX4*)), and ERyfh1 (13). To avoid the accumulation of suppressor mutations in frataxin-deficient cells, the *yfh1* deletion was covered by a shuffle plasmid bearing a wild-type copy of *YFH1* and of *CYH2*. The covering plasmid was ejected before each experiment by plating the cells on YPD and cycloheximide, as described previously (6). Cells overexpressing *MIR1* were transformed with the 2$\mu$ plasmid Yep352-*MIR1*. Unless otherwise stated, cells were grown aerobically in either complete medium (YP-raffinose) or defined medium (6.7 g/liter yeast nitrogen base without amino acids, iron, or copper and containing 0.1% glucose, 2% raffinose, 0.8 g/liter amino acids). The defined media were supplemented with 200 mg/liter adenine, 5 $\mu$M CuSO$_4$, and with various amounts of iron, in the form of ferric citrate (1:20) or ferrous ascorbate (1:10). In some experiments, the cells were grown in defined medium without phosphate (yeast nitrogen base without phosphate), to which various amounts of phosphate was added as K$_2$HPO$_4$/ KH$_2$PO$_4$ (pH 6.5). For conditional expression of *YFH1* by the ERyfh1 strain, the cells were grown in defined medium containing different concentrations of estradiol (0–2.5 nM). The steady-state amount of Yfh1 produced by the cells was proportional to the concentration of estradiol in the medium and was estimated by quantitative immunoblotting (13).

*Cell Fractionation*—Mitochondrial and cytosolic fractions were isolated after treatment of cells with zymolyase, followed by lysis of the protoplasts in 0.6 M sorbitol (buffered with 50 mM Tris, pH 7.8), in the presence of protease inhibitors (protease inhibitor mixture, P8215, Sigma) as described previously (27). The purity of the mitochondrial fraction was estimated by assaying the activity of cytochrome oxidase as described previously (27). Submitochondrial fractionation was carried out as described previously (28).

*Iron and Phosphate Uptake by Isolated Mitochondria*—Mitochondria were suspended at 1 mg/ml in 0.6 M sorbitol buffered with 50 mM HEPES, pH 7, and preincubated at 30 °C for

15 min with 1 mM NADH. For iron uptake experiments, $^{55}$Fe(II)-ascorbate (1:2) was added at a final concentration of 10 $\mu$M. At various time intervals, 100-$\mu$l aliquots were withdrawn and added to ice-cold 0.6 M sorbitol buffered with 50 mM HEPES, pH 7, containing 1 mM unlabeled Fe(II)-ascorbate. The aliquots were washed three times by centrifugation before scintillation counting. For phosphate uptake experiments, the mitochondria were preincubated for 15 min at 30 °C in the same buffer containing 1 mM NADH and 10 $\mu$M Fe(II)-ascorbate, and then 0.5 mM [$^{32}$P]phosphate (as a mix of 1:1 sodium and potassium orthophosphate, pH 7) was added. Aliquots (100 $\mu$l) were withdrawn at intervals and added to ice-cold buffer (sorbitol-HEPES) containing 50 mM unlabeled phosphate. The aliquots were washed three times by centrifugation before scintillation counting.

*Determination of Total, Soluble, and Insoluble Iron and Phosphate in Isolated Mitochondria*—The phosphate content of isolated mitochondria (without prior incubation with [$^{32}$P]phosphate) was determined using a colorimetric molybdate assay (29). Total phosphate was estimated after disrupting whole mitochondria in 10 mM HEPES buffer, pH 7, containing 0.1% SDS. Soluble phosphate was measured as follows; the mitochondria were lysed in hypotonic buffer (10 mM HEPES, pH 7) and sonicated for 30 s; the insoluble fraction was removed by centrifugation at 10,000 $\times$ *g* for 30 min, and the phosphate content of the soluble fraction was measured by the same colorimetric method. Alternatively, the phosphate content and distribution in the mitochondria was determined by scintillation counting after growing the cells in the presence of [$^{32}$P]orthophosphate. Total, soluble, and insoluble iron ($^{55}$Fe) contents in whole mitochondria, in the intermembrane space, and in mitochondrial matrices were measured by scintillation counting of the corresponding fractions.

*Iron Uptake by Whole Cells as a Function of Phosphate Concentration in Medium*—The cells were precultured in defined medium and then transferred to defined medium without phosphate and cultured for a further 15 h. The cells were then harvested, resuspended in the same medium without phosphate at an $A_{600 \, nm}$ of 0.01 and distributed into the wells of a microtiter plate (100 $\mu$l/well). Phosphate (K$_2$HPO$_4$/KH$_2$PO$_4$, pH 7) was added to the wells at various concentrations (0.1 mM-0.2 M), and then iron was added as $^{55}$Fe(II)-ascorbate (1:10). The cells were grown at 30 °C in the microtiter plate with shaking. After 24 h of growth, the $A_{600 \, nm}$ was recorded, and the cells were harvested and washed on the filter of a cell harvester (Brandel) and subjected to scintillation counting.

*RNA Isolation and Real-time Quantitative PCR Analysis*—Total RNA for real-time quantitative PCR analysis was extracted from cells cultured to an $A_{600 \, nm} \sim 0.8$ using the hot phenol method as described previously (30) and purified using Qiagen columns (RNeasy kit). Cultures were done in defined media without phosphate supplemented with 200 mg/l adenine and 50 $\mu$M iron ascorbate, to which 0.1, 10, and 200 mM phosphate was added. Real-time quantitative PCR analysis was performed as described previously (30). The *ACT1* gene mRNA was used for normalization. The primer sequences were as follows: for the *ACT1* gene, 5′-GAGTTGCC-CCAGAAGAACACC-3′ and 5′-GATGGAAACGTAGAAG-
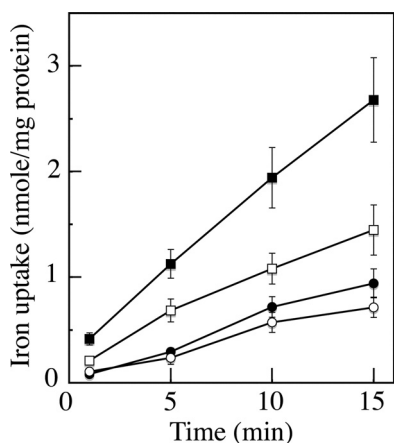
FIGURE 1. **Iron uptake by mitochondria isolated from various strains.** Mitochondria isolated from wild-type (*closed circles*), Δ*mrs3*Δ*mrs4* (*open circles*), Δ*yfh1* (*closed squares*), or Δ*ggc1* (*open squares*) cells grown on complete medium were preincubated for 15 min at 30 °C in 0.6 M sorbitol buffered with 50 mM HEPES, pH 7, containing 1 mM NADH. Then, iron (10 μM $^{55}$Fe(II)-ascorbate) was added. Aliquots were withdrawn at intervals, washed, and counted for iron. Values are means ± S.E. for three experiments.



FIGURE 2. **Dependence of mitochondrial iron uptake on iron concentration.** Mitochondria from wild-type (*circles*) or Δ*yfh1* (*squares*) cells were incubated in the presence of 1 mM NADH in isotonic sorbitol-HEPES buffer at 4 °C (*A*) or 30 °C (*B*) with one of a series of concentrations of $^{55}$Fe(II)-ascorbate for 5 min with (*gray symbols*; nonspecific binding) or without (*black symbols*; total binding) a 1000-fold excess of unlabeled Fe(II)-ascorbate. The mitochondria were washed with isotonic buffer on the filter of a cell harvester before scintillation counting. *Open symbols* represent the specific binding of iron (total binding minus nonspecific binding). Data are from one representative experiment.

GCTGG-3′; for the *FET3* gene, 5′-TAAAGCCGATAACCC-AGGTG-3′ and 5′-CACAGAGCAACTCTGGCAAA-3′; for the *SIT1* gene, 5′-GGCATTTCTTGTTGGATCGT-3′ and 5′-CCAATGATACCGGAATGAGC-3′; for the *PHO84* gene, 5′-CCAAACACAACCACCTTTATTG-3′ and 5′-ACCAGA-TGCAGCAGAAATACC-3′; for the *MIR1* gene, 5′-TGAAT-TTGCTTTCCGGTTTG-3′ and 5′-GGCCAGGAGCCTTCT-TAGTC-3′; for the *PIC2* gene, 5′-GCCAACGAGTCCATGT-CTG-3′ and 5′-CACCATTAACCCATTCCACAA-3′. Relative expression in Δ*yfh1*/WT cells was calculated using the equation described by Pfaffl (31). Results reported were obtained from three biological replicates, and PCR runs were repeated at least twice.

*Miscellaneous*—The in-gel aconitase assay was performed as described previously (32). The respiratory activity of isolated mitochondria was evaluated by an oxypolarographic method. The rate of oxygen consumption was measured with a 1-ml thermostatically controlled oxypolarographic cell equipped with a Clark-type electrode. Low temperature absorption spectra (−191 °C) of whole cells were recorded as described previously (33, 34).

## RESULTS

*Increased Iron Uptake by Isolated Δyfh1 Mitochondria*— Iron is normally stored in the vacuole in yeast (27). Yeast mutants affected in [Fe-S] cluster biogenesis accumulate iron in their mitochondria, and the mechanism by which iron mislocalizes in these mutants is unknown (14). We investigated whether this phenotype of mitochondrial iron accumulation can be detected *in vitro*; we measured iron uptake (from ferrous ascorbate) by mitochondria isolated from different yeast strains (Fig. 1). Mitochondria isolated from a Δ*yfh1* strain accumulated more iron than wild-type mitochondria. This was also true, although to a lesser extent for mitochondria isolated from another mutant affected in [Fe-S] cluster biogenesis, Δ*ggc1* (Fig. 1), which lacks the GTP/GDP mitochondrial carrier (35) and that we used as a control throughout this study
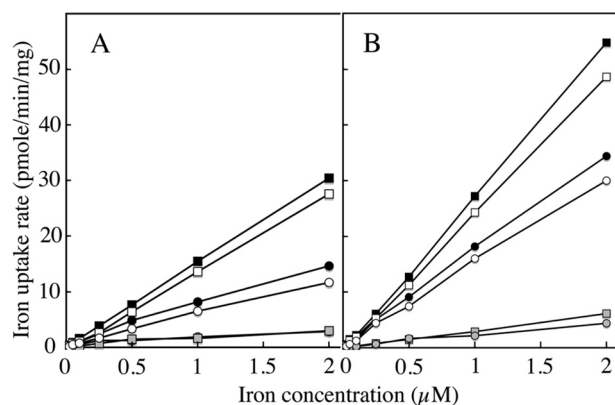
because it accumulates mitochondrial iron in the same form than the Δ*yfh1* mutant (13). However, mitochondria isolated from an Δ*mrs3*Δ*mrs4* strain accumulated similar amounts of iron as wild-type mitochondria (Fig. 1). The *MRS3/4* gene products are generally considered to be the main mitochondrial iron carriers (18) so it is probable that *in vitro* iron uptake observed in this experimental system did not reflect the *in vivo* mechanism of iron acquisition by mitochondria. Moreover, Scatchard experiments did not provide evidence of any saturation for the specific uptake of iron by isolated mitochondria (Fig. 2). Despite this evidence that *in vitro* iron uptake did not mechanistically reflect *in vivo* mitochondrial iron uptake, it is striking that a major phenotype of Δ*yfh1* cells (mitochondrial iron accumulation) was observed when measuring iron uptake by mitochondria isolated from this mutant (Fig. 1). As the mechanism of uptake was not saturable under our experimental conditions (Fig. 2), the greater uptake of iron by Δ*yfh1* mitochondria than by wild-type mitochondria probably did not result from a higher activity of the mitochondrial iron carrier(s) involved in these experiments. Another possibility is that, in Δ*yfh1* but not in wild-type mitochondria, iron loses its mobility after entering the mitochondria, thereby displacing the thermodynamic equilibrium toward increased net intramitochondrial iron accumulation. This would be consistent with the observation that, in Scatchard experiments (Fig. 2), the mean rate of iron uptake by wild-type mitochondria increased about three times when the temperature was increased from 4 °C (Fig. 2*A*) to 30 °C (Fig. 2*B*). In the same conditions, the rate of iron uptake by Δ*yfh1* only doubled (Fig. 2). This suggests that one component of the iron uptake process that is temperature-independent is greater for Δ*yfh1* than wild-type mitochondria. This component may be iron precipitation inside the mitochondria. We tested this possibility by investigating the fate of iron after its uptake by mitochondria isolated from different strains.
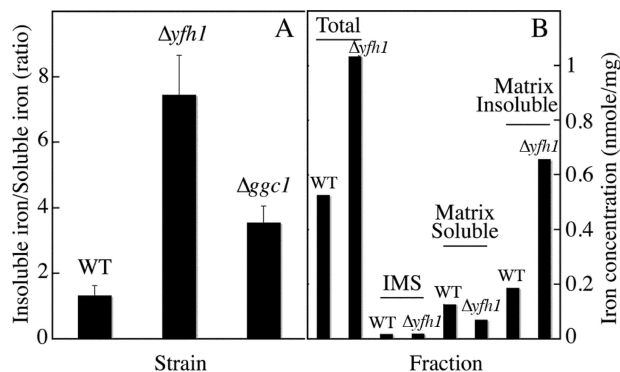
FIGURE 3. **Iron precipitation in the matrix of Δ*yfh1* mitochondria.** *A*, ratio of insoluble-to-soluble iron in whole mitochondria of wild-type, Δ*yfh1*, and Δ*ggc1* cells. The mitochondria (1 mg/ml) were incubated for 30 min at 30 °C in 0.6 M sorbitol buffered with 50 mM HEPES, pH 7, containing 1 mM NADH and 10 μM $^{55}$Fe(II)-ascorbate, washed in isotonic buffer, and then lysed in hypotonic buffer and sonicated. The soluble and insoluble fractions were separated by centrifugation before counting iron in each fraction. Data are means ± S.E. for three experiments. *B*, intramitochondrial distribution of soluble and insoluble iron in WT and Δ*yfh1* mitochondria. The mitochondria (1 mg/ml) were incubated for 5 min at 30 °C in 0.6 M sorbitol buffered with 50 mM HEPES, pH 7, containing 1 mM NADH and 10 μM $^{55}$Fe(II)-ascorbate, washed in isotonic buffer, and fractionated as described under "Experimental Procedures." The soluble and insoluble fractions of the intermembrane space (*IMS*) and of the matrix were separated by centrifugation before counting iron in each fraction. Data are from one representative experiment.

*Precipitation of Iron in Δyfh1 Mitochondrial Matrix*—Mutants affected in [Fe-S] cluster biogenesis accumulate iron in the mitochondria essentially in an insoluble form, as ferric phosphate nanoparticles (6, 13, 20, 21). We tested whether the apparent higher rate of iron uptake by mitochondria isolated from Δ*yfh1* cells was associated with precipitation of iron *in vitro* in the mitochondrial matrix. Mitochondria were incubated with $^{55}$Fe (as ferrous ascorbate), washed, and then disrupted by sonication in hypotonic buffer. The lysates were then separated into soluble and insoluble fractions by ultracentrifugation. Iron was determined in each of these fractions (Fig. 3*A*). In Δ*yfh1* mitochondria, but not in wild-type mitochondria, most of the iron precipitated and became insoluble rapidly after its uptake. The same process occurred in Δ*ggc1* mitochondria, although to a lesser extent (Fig. 3*A*). Analysis of the submitochondrial fractions showed that iron precipitated in the mitochondrial matrix of Δ*yfh1* mitochondria (Fig. 3*B*). The precipitation of iron in the matrix of Δ*yfh1* mitochondria presumably results from its oxidation to ferric ions in this compartment and binding to an anion with which it forms an insoluble complex. It is plausible that the ferrous iron is oxidized by oxygen, and the resulting ferric ions precipitate with phosphate, which was shown previously to be associated with insoluble mitochondrial iron in Δ*yfh1* cells *in vivo* (6, 13).

*Role of Oxygen and Phosphate in Iron Precipitation*—Iron did not accumulate in the mitochondria of Δ*yfh1* cells grown anaerobically (2 ppm of O$_2$). Mitochondria isolated from aerobically grown Δ*yfh1* cells and incubated with iron (as ferrous ascorbate) under anaerobiosis also did not precipitate iron in the matrix (data not shown). However, addition of ferrous ascorbate to a suspension of isolated Δ*yfh1* mitochondria under aerobiosis resulted in significant oxygen consumption by the mitochondria (Fig. 4) consistent with the oxidation of iron
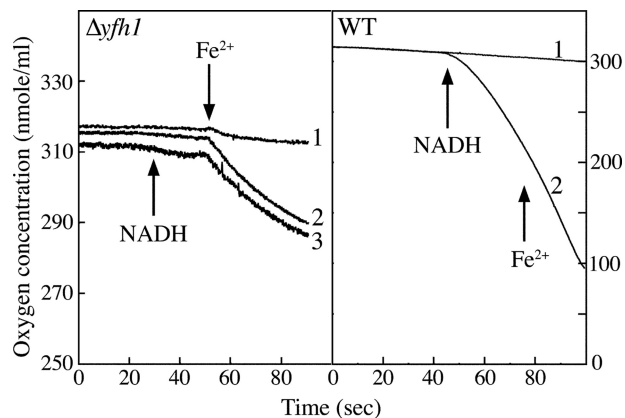


FIGURE 4. **Effect of ferrous iron on oxygen consumption by isolated mitochondria.** Mitochondria from Δ*yfh1* (*left panel*) or wild-type cells (*right panel*) were suspended at 2 mg/ml in sorbitol-HEPES isotonic buffer at 30 °C in the chamber of the oxypolarographic cell, and oxygen consumption was recorded. At the indicated times, NADH (1 mM) and Fe(II)-ascorbate (50 μM) were added. *Left panel*: curve 1, addition of Fe(II)-ascorbate to the buffer alone (with NADH but without mitochondria); *curve 2*, addition of Fe(II)-ascorbate to the suspension of Δ*yfh1* mitochondria (without NADH); *curve 3*, addition of Fe(II)-ascorbate to the suspension of Δ*yfh1* mitochondria (with prior addition of NADH). *Right panel*: curve 1, addition of Fe(II)-ascorbate to the suspension of wild-type mitochondria (without NADH); *curve 2*, addition of Fe(II)-ascorbate to the suspension of wild-type mitochondria (with prior addition of NADH).
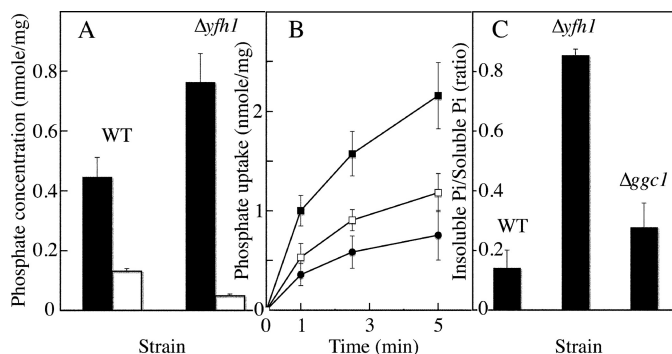


FIGURE 5. **Phosphate content, uptake, and distribution in the mitochondria of various strains.** *A*, Total (*black bars*) and soluble (*white bars*) phosphate measured colorimetrically in mitochondria of wild-type and Δ*yfh1* cells grown on complete medium (YP-raffinose). Values are means ± S.E. for three experiments. *B*, kinetics of phosphate uptake by isolated mitochondria. Mitochondria isolated from wild-type (*closed circles*), Δ*yfh1* (*closed squares*) or Δ*ggc1* (*open squares*) cells grown on complete medium were preincubated for 15 min at 30 °C in 0.6 M sorbitol buffered with 50 mM HEPES, pH 7, containing 1 mM NADH, and then phosphate was added as 500 μM [$^{32}$P]orthophosphate. Aliquots were withdrawn at intervals, washed, and counted for phosphate. Values reported are means ± S.E. for three experiments. *C*, ratio of insoluble-to-soluble phosphate in whole mitochondria from wild-type, Δ*yfh1*, and Δ*ggc1* cells. The mitochondria (1 mg/ml) were incubated for 30 min at 30 °C in 0.6 M sorbitol buffered with 50 mM HEPES, pH 7, containing 1 mM NADH and 500 μM [$^{32}$P]orthophosphate, washed in isotonic buffer, and then lysed in hypotonic buffer and sonicated. The soluble and insoluble fractions were separated by centrifugation before counting phosphate in each fraction. Values are means ± S.E. for three experiments. *Pi*, inorganic phosphate.

in the mitochondrial matrix. A good candidate anion for precipitating the resulting ferric iron is phosphate. We used a colorimetric method to assay the phosphate content of Δ*yfh1* and wild-type mitochondria after cell growth in complete medium (YP-raffinose). There was significantly more total phosphate but much less soluble phosphate in Δ*yfh1* mitochondria than in wild-type mitochondria (Fig. 5*A*). Similar results were obtained by growing the cells in complete medium containing

[³²P]orthophosphate and then counting soluble and insoluble phosphate in the mitochondria; the insoluble-to-soluble ratio of phosphate in the mitochondria measured by this method was $2.0 \pm 0.3$ for the wild-type, $8.7 \pm 0.5$ for $\Delta yfh1$ and $4.3 \pm 0.9$ for $\Delta ggc1$ mitochondria (mean $\pm$ S.E. for three experiments). The rate of orthophosphate uptake was also higher by isolated $\Delta yfh1$ than isolated wild-type or $\Delta ggc1$ mitochondria (Fig. 5*B*). We then checked whether phosphate precipitated *in vitro* in the matrix of mitochondria isolated from $\Delta yfh1$ cells. Isolated mitochondria were incubated with ferrous ascorbate and [³²P]orthophosphate. Most of the phosphate taken up by wild-type mitochondria remained soluble, whereas a significant part of the phosphate in $\Delta yfh1$ mitochondria was recovered in the insoluble fraction (Fig. 5*C*). Much less phosphate precipitated in $\Delta ggc1$ than in $\Delta yfh1$ mitochondria (Fig. 5*C*). These various findings suggest that iron and phosphate co-precipitate in the mitochondria of mutants defective in [Fe-S] cluster biogenesis, both *in vivo* and *in vitro*, and that this phenomenon is more extensive in $\Delta yfh1$ mitochondria than in mitochondria of another [Fe-S] cluster biogenesis mutant ($\Delta ggc1$). We examined the development of iron and phosphate precipitation *in vivo*, in a strain with conditional expression of *YFH1*. For this experiment, we used the ERyfh1 in which transcription of the *YFH1* gene is controlled by the concentration of estradiol in the growth medium (13). We previously showed that with 2.5 nM estradiol in the medium, the amount of Yfh1 was ~100 molecules per cell (*i.e.* >10-fold less than in wild-type cells), which was enough to prevent mitochondrial iron accumulation (13). We thus analyzed ERyfh1 cells grown with estradiol in the medium at concentrations ranging from 0 to 2.5 nM (0, 0.5, 1, and 2.5 nM), leading to cellular Yfh1 contents ranging from 0 to 100 molecules per cell. At 2.5 nM estradiol, the mitochondrial phosphate and iron contents and distributions in the ERyfh1 strain were similar to the values found in the wild-type strain (data not shown). Fig. 6 shows that the insoluble-to-soluble ratio of mitochondrial iron progressively increased when the estradiol concentration in the medium was decreased from 2.5 to 0 nM. In the same conditions, the insoluble-to-soluble ratio of phosphate in the mitochondria suddenly increased (from about two to eight; Fig. 6) when the estradiol concentration was decreased from 2.5 to 1 nM, a condition in which iron accumulation was still mild, and then increased moderately when estradiol concentration was further decreased (Fig. 6). This result indicates that phosphate precipitation occurred very early, when iron just started to accumulate moderately in the mitochondria.

*High Phosphate Concentration in Medium Suppresses Iron Accumulation Phenotype of $\Delta yfh1$ Cells*—Co-precipitation of iron and phosphate in the mitochondria of $\Delta yfh1$ cells theoretically has several possible implications. One is that excess phosphate in the mitochondria is part of the cause of iron precipitation leading to iron accumulation in the mitochondria. In this case, it should be possible to decrease iron accumulation in the mitochondria by decreasing the cell phosphate content. Another possibility is that co-precipitation with iron reduces the amount of free phosphate available for oxidative phosphorylation in the mitochondrial matrix of
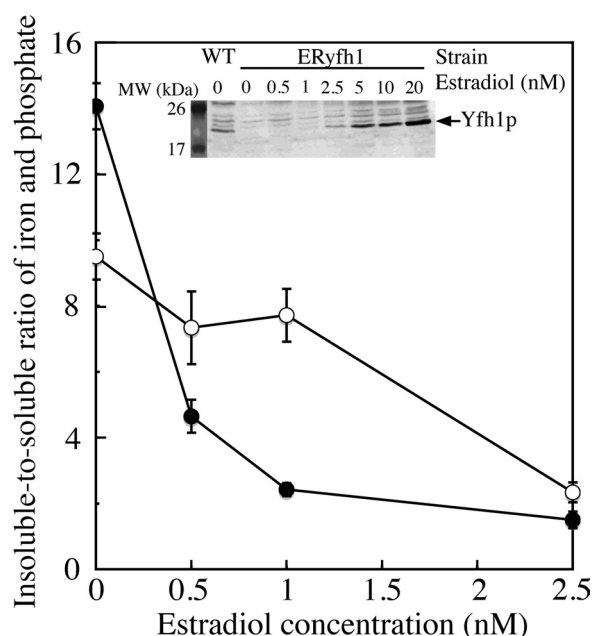


FIGURE 6. **Iron and phosphate solubility in the mitochondria of a conditional *yfh1* mutant grown in different conditions.** Ratios of insoluble-to-soluble iron (*closed symbols*) and phosphate (*open symbols*) in whole mitochondria of the ERyfh1 strain were determined after growing the cells with estradiol at concentration in the range 0–2.5 nM (leading to an estimated steady-state level of Yfh1 of 0–100 molecules Yfh1 per cell). *Inset*, estradiol-dependent production of Yfh1p. The amount of Yfh1p produced in WT and ERyfh1 cells grown with 0–2.5 nM estradiol was assessed by Western blotting (20 μg mitochondrial protein per lane). Yfh1p was no longer detectable at concentrations of estradiol lower than 1 nM, and its level was estimated by linear regression from standard curves. Values are means $\pm$ S.E. for three experiments. *MW*, molecular mass.
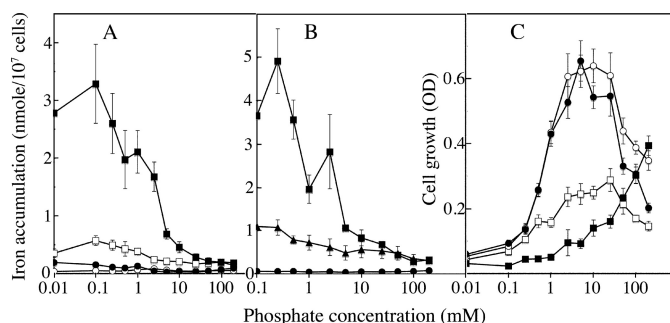


FIGURE 7. **Effect of phosphate concentration on iron accumulation and growth of various strains.** *A*, iron accumulation by wild-type (*circles*) or $\Delta yfh1$ (*squares*) cells grown with each of a series of concentrations of phosphate and with either 1 μM (*open symbols*) or 50 μM (*closed symbols*) iron (as ⁵⁵Fe(II)-ascorbate). *B*, iron accumulation by wild-type (*circles*), $\Delta yfh1$ (*squares*), or $\Delta ggc1$ (*triangles*) cells grown with each of a series of concentrations of phosphate and with 50 μM iron (as ⁵⁵Fe(II)-ascorbate). *C*, growth of wild-type (*circles*) or $\Delta yfh1$ (*squares*) cells grown with each of a series of concentrations of phosphate and with either 1 μM (*open symbols*) or 50 μM (*closed symbols*) iron (as Fe(II)-ascorbate). The cell growth was estimated by measuring the OD 600 nm in microtiter plates (optical path of 0.1 cm). Reported values are means $\pm$ S.E. for four experiments.

$\Delta yfh1$ cells. Were this the case, increasing the cell phosphate content would be beneficial, by making more phosphate available for biological processes. We studied the effect of phosphate concentration in the growth medium on cell growth and on iron accumulation by the cells (Fig. 7). Increasing the phosphate concentration in the medium resulted in a substantial decrease in iron accumulation by $\Delta yfh1$ cells, which recovered wild-type levels of iron at a phosphate concentra-

**TABLE 1**

Relative abundance of some transcripts in Δ*yfh1* cells compared to wild-type cells grown in defined medium containing different concentrations of phosphate. Transcript abundance was estimated by real-time quantitative PCR analysis, as described under "Experimental Procedures." Results are expressed as the ratio of transcript abundance in Δ*yfh1* cells *versus* wild-type cells. Values are means ± S.E. for three experiments.

| Gene | Phosphate concentration | | |
| --- | --- | --- | --- |
| | 0.1 mM | 10 mM | 200 mM |
| *FET3* | 129.6 ± 14.24 | 24.9 ± 2.09 | 8.3 ± 0.91 |
| *SIT1* | 194.8 ± 20.31 | 89.6 ± 4.3 | 27.5 ± 2.65 |
| *PHO84* | 4.3 ± 0.15 | 1.3 ± 0.12 | 1.3 ± 0.29 |
| *MIR1* | 0.6 ± 0.03 | 0.5 ± 0.09 | 1.1 ± 0.09 |
| *PIC2* | 0.1 ± 0.01 | 0.9 ± 0.16 | 2.8 ± 0.18 |

tion of 200 mM (Fig. 7*A*). In parallel with this effect, Δ*yfh1* cell growth was strongly stimulated by high concentrations of phosphate in the medium (Fig. 7*C*). This effect of phosphate was iron-dependent, being more pronounced when the medium contained excess iron (50 μM) (Fig. 7, *A* and *C*), and was much larger for Δ*yfh1* cells than for another mutant defective in [Fe-S] cluster biogenesis (Δ*ggc1*; Fig. 7*B*). The beneficial effect of phosphate on Δ*yfh1* cell physiology was also evidenced by the observation that in the presence of excess phosphate in the medium (100 mM), Δ*yfh1* cells recovered some ability to grow on a nonfermentable carbon source (YP-glycerol plate), indicating that the cells recovered some respiratory activity in this condition (data not shown). The effect of phosphate in the medium on mitochondrial iron accumulation was probably mostly transcriptional because the expression of genes of the iron regulon (*FET3* and *SIT1*, regulated by Aft1) in Δ*yfh1* cells was strongly decreased when the concentration of phosphate in the medium was increased from 0.1 to 200 mM (Table 1). Table 1 also shows that *MIR1* and *PIC2*, encoding the main mitochondrial phosphate carriers, were repressed in Δ*yfh1 cells* (compared with wild-type cells) grown on low phosphate medium. Expression of these genes in Δ*yfh1* cells increased when increasing the phosphate content of the medium (Table 1), which, together with the decrease in iron accumulation by the cells, could account for the better fitness of Δ*yfh1* cells grown in phosphate-rich medium.

*Overexpression of Mitochondrial Phosphate Carrier Mir1 Improves Growth and Respiratory Functions of Δyfh1 Cells*— Our results suggest that although total phosphate is more abundant in Δ*yfh1* than wild-type mitochondria, Δ*yfh1* cells suffer from a lack of bioavailable phosphate due to its co-precipitation with iron. In agreement with this hypothesis, we observed that the expression of *PHO84*, encoding the high affinity phosphate transporter, was strongly increased in Δ*yfh1* cells (compared with wild-type cells) in low phosphate medium (Table 1). Mir1 is the main mitochondrial phosphate carrier in yeast, although Pic2 also contributes to mitochondrial phosphate import under stress conditions (22). We tried to manipulate the mitochondrial phosphate content/availability by overexpressing *MIR1* on a multicopy plasmid in wild-type, Δ*yfh1*, and Δ*ggc1* strains. When *MIR1* was overexpressed, the steady-state level of soluble mitochondrial phosphate increased only moderately (23 ± 4% in wild-type mitochondria and 8 ± 2% in Δ*yfh1* mitochondria; mean ± S.E. for three experiments). However, overexpression of *MIR1*
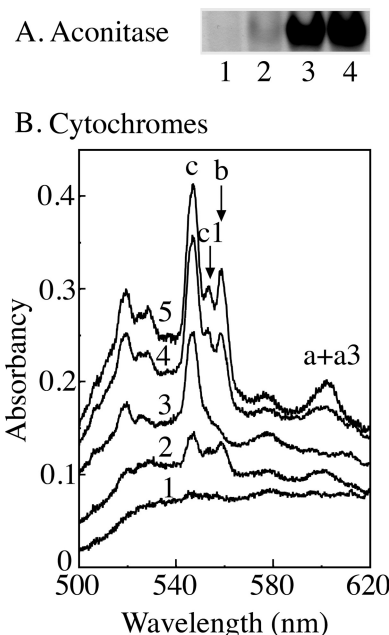


FIGURE 8. **Improvement of mitochondrial functions by *MIR1* overexpression in Δ*yfh1* cells.** *A*, in-gel aconitase activity (using 50 μg mitochondrial protein per lane). *Lane 1*, Δ*yfh1*; *lane 2*, Δ*yfh1-MIR1*; *lane 3*, WT; *lane 4*, WT-*MIR1*. *B*, low temperature spectra of whole cells. *Curve 1*, Δ*yfh1*; *curve 2*, Δ*yfh1-MIR1*; *curve 3*, Δ*ggc1-MIR1*; *curve 4*, Δ*ggc1*; *curve 5*, WT.
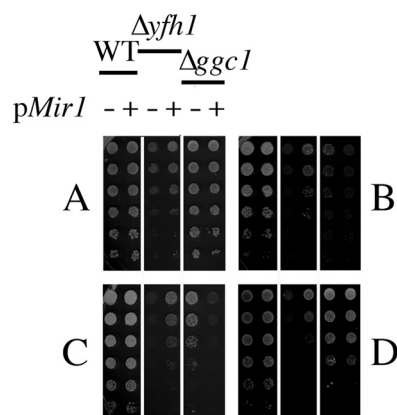


FIGURE 9. **Effect of *MIR1* overexpression on cell growth in various conditions.** Wild-type, Δ*yfh1*, and Δ*ggc1* cells were transformed by the Yep352-*MIR1* plasmid (p*MIR1* +) or by the empty plasmid (p*MIR1* −). The cells were sequentially diluted 5-fold and then plated on various media. *A*, defined medium; *B*, YP-glycerol; *C*, YP-glycerol and 100 μM Fe(III)-citrate; *D*, defined medium and 0.5 mM CuSO_4.

in Δ*yfh1* cells, but not that in Δ*ggc1* cells, clearly resulted in an improvement of cell growth and of the mitochondrial functions that are impaired in the frataxin-deficient mutant. Both cytochrome synthesis and [Fe-S] cluster biogenesis (as evidenced by measuring aconitase activity) were improved in Δ*yfh1* cells by overexpression of *MIR1* (Fig. 8, *A* and *B*). In contrast, when *MIR1* was overexpressed in Δ*ggc1* cells, the synthesis of cytochromes was impaired (cytochromes *b* and $c_1$ disappeared) (Fig. 8*B*), indicating that the beneficial effect of *MIR1* overexpression was specific to Δ*yfh1* cells. Moreover, growth of the Δ*yfh1* cells but not of Δ*ggc1* cells on a nonfermentable carbon source was partly restored by *MIR1* overexpression (Fig. 9, *B* and *C*: compare *lanes 3* and *4* (Δ*yfh1*) and *lanes 5* and *6* (Δ*ggc1*)). The resistance of the cells to an oxida-

tive stress (copper) was also improved when *MIR1* was over-expressed in the Δ*yfh1* mutant (Fig. 9*D*, *lanes 3* and *4*), but not in the Δ*ggc1* mutant (Fig. 9*D*, *lanes 5* and *6*). Suppressor mutations are frequent in Δ*yfh1* cells (6), so we checked that the effects of *MIR1* overexpression in Δ*yfh1* cells were reversible by ejecting the plasmid bearing *MIR1* (and *URA3* as the selection marker) on 5-fluoroorotic acid plates. The phenotype of Δ*yfh1* cells from which the *MIR1* plasmid was ejected was the same as the phenotype of untransformed Δ*yfh1* cells (data not shown). This demonstrates that the improvement of respiratory functions observed in Δ*yfh1* cells overexpressing *MIR1* was not due to any suppressor mutations.

## DISCUSSION

*Physiological Implications of Iron Accumulation and Precipitation in Δyfh1 Mitochondria*—Frataxin-deficient yeast cells accumulate iron in the mitochondria in the form of amorphous nanoparticles of ferric phosphate, as do other mutants defective in [Fe-S] cluster biogenesis or export (6, 13, 20, 21). This observation has several implications. First, as most of the iron accumulated in the mitochondria is biologically unavailable/inactive, these mutants might paradoxically suffer from a lack of iron, despite being overloaded with iron. Consistent with this, the viability of Δ*yfh1* cells was increased when an excess iron was added to the medium (13). A second implication is that these cells must be affected in their metabolism of phosphate because a large amount of phosphate co-precipitates with iron in the mitochondria and thereby becomes unavailable for vital biological processes, including oxidative phosphorylation. The issue of iron accumulation/precipitation in Δ*yfh1* mitochondria has been extensively studied but that of phosphate co-precipitation in these mitochondria has never been investigated, as far as we are aware. Nevertheless, there should be a link between phosphate and iron homeostasis in yeast because iron and other cations are normally stored in the vacuole of this organism in association with polyphosphates (27). The effect of phosphate on metal ion homeostasis in yeast was recently investigated by Rosenfeld *et al.* (26), who found that disruptions in phosphate control elicit an Aft1-dependent iron starvation response. In Δ*yfh1* mutants, iron is not stored in the vacuole but accumulates in the mitochondria, and here also, iron is associated with phosphate. Unlike the iron stored in vacuoles of wild-type cells, the iron accumulated in mitochondria of mutant cells cannot be mobilized because it forms an amorphous precipitate of ferric phosphate. Here, we show that a similar process occurs *in vitro*; both orthophosphate anions and ferrous cations that are taken up by isolated Δ*yfh1* mitochondria rapidly become insoluble in the mitochondrial matrix. The most probable explanation is that the iron is oxidized and then precipitates with phosphate inside the mitochondria.

*Cause of Iron and Phosphate Co-precipitation*—The reason why this process occurs in frataxin-deficient mitochondria but not in wild-type mitochondria might be related to the presence, in Δ*yfh1* mitochondria, of preformed nanoparticles of ferric phosphate; these nanoparticles may act as nucleation centers for further precipitation of iron and phosphate. It is particularly striking that this phenotype observed *in vivo* in Δ*yfh1* cells is also found *in vitro* with isolated Δ*yfh1* mitochondria, although there is no evidence that the same mechanism is at play.

One hypothesis is that iron accumulation/precipitation *in vivo* in Δ*yfh1* mitochondria is a result of phosphate accumulation, which itself would result from deficiencies in the respiratory chain, with a subsequent decrease in the flux of phosphate utilization for oxidative phosphorylation. Iron entering the mitochondria may precipitate with this excess phosphate, after oxidation by oxygen, the concentration of which is expected to be higher in mutant than in wild-type mitochondria. In this hypothesis, phosphate would accumulate first in Δ*yfh1* mitochondria, followed by iron precipitation due to the excess of phosphate. To address this issue, we tried to determine the time course of iron and phosphate accumulation/precipitation in the mitochondria when the level of Yfh1 was progressively decreased in a strain expressing *YFH1* conditionally. Our data show that phosphate precipitates very early when the level of Yfh1 is decreased, whereas iron accumulation and precipitation is more progressive. Thus, iron probably precipitates in the form of ferric phosphate as soon as it starts to accumulate in the mitochondria, resulting in a rapid decrease in the soluble, bioavailable pool of phosphate. When we progressively decreased the level of Yfh1, we did not observe any transient increase in the soluble phosphate pool preceding the accumulation/precipitation of iron. Thus, our data do not allow us to conclude that iron precipitation in frataxin-deficient cells is initially caused by the presence of excess phosphates in the mitochondria of these cells. Moreover, if this was the case, iron accumulation/precipitation in Δ*yfh1* cells would be expected to be decreased by phosphate-limiting conditions, which is the opposite of what we found. Further investigations are thus needed to identify the cause of iron and phosphate accumulation and co-precipitation. Possibly, iron starts to accumulate because it cannot be incorporated properly in heme and [Fe-S] clusters, and it oxidizes and co-precipitates with phosphate as a result of the low capacity of the mutant mitochondria to reduce oxygen.

*Beneficial Effects of Excess Phosphate in Medium and of MIR1 Overexpression*—Iron accumulation in Δ*yfh1* cells strongly increased with decreased concentrations of phosphate in the medium, and conversely, growing the cells in the presence of a large excess of phosphate resulted in much less iron accumulation. The relationship between phosphate and iron homeostasis is thus complex because excess phosphate improves the fitness of Δ*yfh1* cells in terms of growth, iron accumulation and the ability of the cells to grow on a nonfermentable carbon source. This effect is probably mostly transcriptional because increasing phosphate concentration in the medium leads to a decrease in the level of transcription of Aft1-regulated genes, which are constitutively induced in mutants affected in [Fe-S] cluster assembly. But here again, the effect of phosphate could be indirect. We showed here that excess phosphate in the medium resulted in increased fitness of Δ*yfh1* cells, which recovered some ability to grow on a nonfermentable carbon source. Excess phosphate in the medium also resulted in increased expression of the genes encoding the mitochondrial phosphate carriers, *MIR1* and *PIC2.* In sep-

arate experiments, we showed that overexpressing *MIR1* without changing the phosphate content of the medium also improved the respiratory functions of Δ*yfh1* cells. Thus, the most probable explanation is that the mitochondrial functions of frataxin-deficient cells are partially restored by increasing the level of bioavailable phosphate in the mitochondria. Such an improvement of the respiratory functions, involving some restoration of mitochondrial [Fe-S] biogenesis, is itself expected to decrease the level of transcription of the iron regulon genes, leading to decreased iron accumulation.

We suggest that Δ*yfh1* cells suffer from a lack of available phosphate for biological processes, in exactly the same way as they suffer from a lack of bioavailable iron, because iron and phosphate co-precipitate in the mitochondria by a mechanism that remains to be elucidated. Frataxin-deficient cells are impaired in oxidative phosphorylation (36), and there are several possible causes of this defect, including insufficient available inorganic phosphate.

Frataxin-deficient cells suffer from multiple defects, which are probably cumulative and generate vicious spirals. For example, a primary small defect in [Fe-S] cluster assembly could result in iron accumulation/precipitation in the mitochondria, leading to decreased iron availability (including for [Fe-S] biogenesis) thereby continuing the spiral. The same could be true for phosphate; the defect in oxidative phosphorylation resulting from the deficiencies in the respiratory chain may be strengthened by the lack of phosphate resulting from the co-precipitation of iron and phosphate in the matrix. This obviously remains a hypothesis, and further evidence is required.

The beneficial effect of increasing phosphate concentration in the medium was much clearer in the Δ*yfh1* mutant than in the Δ*ggc1* mutant that we used as a control. Both mutants are affected in [Fe-S] cluster assembly and accumulate iron in the mitochondria in the same form of nanoparticles of ferric phosphate (13). Several phenotypes found in frataxin-deficient cells are shared by different mutants affected in the biogenesis of [Fe-S] clusters, and it is thus important to compare different [Fe-S] mutants to determine which phenotypes are specifically related to the lack of frataxin rather than to a general defect in [Fe-S] biogenesis. Here, we observed some co-precipitation of iron and phosphate in both Δ*yfh1* and Δ*ggc1* mitochondria, although this phenotype was much more marked in Δ*yfh1* than in Δ*ggc1* mitochondria. Similarly, increasing the phosphate concentration in the medium resulted in decreased iron accumulation in both mutants, but this effect was again much more spectacular in Δ*yfh1* than in Δ*ggc1* cells. These differences between the mutants might be due to the fact that the phenotypes of iron accumulation and of respiration deficiency are more pronounced in Δ*yfh1* than in Δ*ggc1* cells. However, the beneficial effect of *MIR1* overexpression was not observed at all in the Δ*ggc1* mutant, thereby suggesting a specific effect of phosphate in frataxin-deficient cells. Our interpretation of these various findings is that Mir1 overproduction makes phosphate more available for biological processes in the mitochondrial matrix of Δ*yfh1* mitochondria (where most of the phosphate present is precipitated and biologically unavailable), thereby improving mitochondrial functions in a way that remains to be elucidated. Alterna-

tively, the mitochondrial functions of Δ*yfh1* cells might be improved by the increased flux of phosphate into the mitochondria because Mir1-mediated phosphate import into mitochondria significantly contributes to the mitochondrial membrane potential (37). We are currently testing these hypotheses.

## REFERENCES

1. Campuzano, V., Montermini, L., Moltò, M. D., Pianese, L., Cossée, M., Cavalcanti, F., Monros, E., Rodius, F., Duclos, F., Monticelli, A., Zara, F., Cañizares, J., Koutnikova, H., Bidichandani, S. I., Gellera, C., Brice, A., Trouillas, P., De Michele, G., Filla, A., De Frutos, R., Palau, F., Patel, P. I., Di Donato, S., Mandel, J. L., Cocozza, S., Koenig, M., and Pandolfo, M. (1996) *Science* **271,** 1423–1427
2. Gerber, J., Mühlenhoff, U., and Lill, R. (2003) *EMBO Rep.* **4,** 906–911
3. Li, H., Gakh, O., Smith, D. Y., 4th, and Isaya, G. (2009) *J. Biol. Chem.* **284,** 21971–21980
4. Santos, R., Lefevre, S., Sliwa, D., Seguin, A., Camadro, J. M., and Lesuisse, E. (2010) *Antioxid. Redox. Signal* **13,** 651–690
5. Stemmler, T. L., Lesuisse, E., Pain, D., and Dancis, A. (2010) *J. Biol. Chem.* **285,** 26737–26743
6. Lesuisse, E., Santos, R., Matzanke, B. F., Knight, S. A., Camadro, J. M., and Dancis, A. (2003) *Hum. Mol. Genet.* **12,** 879–889
7. Yoon, T., and Cowan, J. A. (2004) *J. Biol. Chem.* **279,** 25943–25946
8. Chantrel-Groussard, K., Geromel, V., Puccio, H., Koenig, M., Munnich, A., Rötig, A., and Rustin, P. (2001) *Hum. Mol. Genet.* **10,** 2061–2067
9. Calabrese, V., Lodi, R., Tonon, C., D'Agata, V., Sapienza, M., Scapagnini, G., Mangiameli, A., Pennisi, G., Stella, A. M., and Butterfield, D. A. (2005) *J. Neurol. Sci.* **233,** 145–162
10. Armstrong, J. S., Khdour, O., and Hecht, S. M. (2010) *FASEB J.* **24,** 2152–2163
11. Santos, M. M., Ohshima, K., and Pandolfo, M. (2001) *Hum. Mol. Genet.* **10,** 1935–1944
12. Cavadini, P., Gellera, C., Patel, P. I., and Isaya, G. (2000) *Hum. Mol. Genet.* **9,** 2523–2530
13. Seguin, A., Sutak, R., Bulteau, A. L., Garcia-Serres, R., Oddou, J. L., Lefevre, S., Santos, R., Dancis, A., Camadro, J. M., Latour, J. M., and Lesuisse, E. (2010) *Biochim. Biophys. Acta.* **1802,** 531–538
14. Philpott, C. C., and Protchenko, O. (2008) *Eukaryot. Cell* **7,** 20–27
15. Li, L., and Kaplan, J. (1997) *J. Biol. Chem.* **272,** 28485–28493
16. Froschauer, E. M., Schweyen, R. J., and Wiesenberger, G. (2009) *Biochim. Biophys. Acta* **1788,** 1044–1050
17. Foury, F., and Roganti, T. (2002) *J. Biol. Chem.* **277,** 24475–24483
18. Mühlenhoff, U., Stadler, J. A., Richhardt, N., Seubert, A., Eickhorst, T., Schweyen, R. J., Lill, R., and Wiesenberger, G. (2003) *J. Biol. Chem.* **278,** 40612–40620
19. Zhang, Y., Lyver, E. R., Knight, S. A., Pain, D., Lesuisse, E., and Dancis, A. (2006) *J. Biol. Chem.* **281,** 22493–22502
20. Miao, R., Martinho, M., Morales, J. G., Kim, H., Ellis, E. A., Lill, R., Hendrich, M. P., Münck, E., and Lindahl, P. A. (2008) *Biochemistry* **47,** 9888–9899
21. Miao, R., Kim, H., Koppolu, U. M., Ellis, E. A., Scott, R. A., and Lindahl, P. A. (2009) *Biochemistry* **48,** 9556–9568
22. Hamel, P., Saint-Georges, Y., de Pinto, B., Lachacinski, N., Altamura, N., and Dujardin, G. (2004) *Mol. Microbiol.* **51,** 307–317
23. Takabatake, R., Siddique, A. B., Kouchi, H., Izui, K., and Hata, S. (2001) *J. Biochem.* **129,** 827–833
24. Murakami, H., Blobel, G., and Pain, D. (1990) *Nature* **347,** 488–491
25. Schroers, A., Krämer, R., and Wohlrab, H. (1997) *J. Biol. Chem.* **272,** 10558–10564
26. Rosenfeld, L., Reddi, A. R., Leung, E., Aranda, K., Jensen, L. T., and Culotta, V. C. (2010) *J. Biol. Inorg. Chem.* **15,** 1051–1062
27. Raguzzi, F., Lesuisse, E., and Crichton, R. R. (1988) *FEBS Lett.* **231,** 253–258
28. Martin, H., Eckerskorn, C., Gärtner, F., Rassow, J., Lottspeich, F., and Pfanner, N. (1998) *Anal. Biochem.* **265,** 123–128
29. Reddi, A. R., Jensen, L. T., Naranuntarat, A., Rosenfeld, L., Leung, E.,

Shah, R., and Culotta, V. C. (2009) *Free Radic. Biol. Med.* **46,** 154–162

30. Auchère, F., Santos, R., Planamente, S., Lesuisse, E., and Camadro, J. M. (2008) *Hum. Mol. Genet.* **17,** 2790–2802
31. Pfaffl, M. W. (2001) *Nucleic Acids Res.* **29,** e45
32. Amutha, B., Gordon, D. M., Gu, Y., Lyver, E. R., Dancis, A., and Pain, D. (2008) *J. Biol. Chem.* **283,** 1362–1371
33. Labbe, P., and Chaix, P. (1969) *Bull. Soc. Chim. Biol.* **51,** 1642–1644
34. Labbe, P., and Chaix, P. (1971) *Anal. Biochem.* **39,** 322–326
35. Vozza, A., Blanco, E., Palmieri, L., and Palmieri, F. (2004) *J. Biol. Chem.* **279,** 20850–20857
36. Ristow, M., Pfister, M. F., Yee, A. J., Schubert, M., Michael, L., Zhang, C. Y., Ueki, K., Michael, M. D., 2nd, Lowell, B. B., and Kahn, C. R. (2000) *Proc. Natl. Acad. Sci. U.S.A.* **97,** 12239–12243
37. Zara, V., Dietmeier, K., Palmisano, A., Vozza, A., Rassow, J., Palmieri, F., and Pfanner, N. (1996) *Mol. Cell. Biol.* **16,** 6524–6531